25TH INTERNATIONAL NORTH SEA FLOW MEASUREMENT WORKSHOP
16th to 19th October 2007, Oslo, Norway

A New Approach to MPFM Performance Assessment in Heavy Oil

Martin Basil, SOLV Limited
Gordon Stobie, ConocoPhillips
Winsor Letton, Letton-Hall Group

1 Abstract

The performance of a MPFM (Multi Phase Flow Meter) is normally assessed with an observational data model obtained by comparison with a reference meter. Typically the vendor will provide the performance from their own databases using data from a wide range of sources including JIP's, client sponsored trials, field trials and the vendors own calibration facilities. This data is processed to model the MPFM and compiled into databases over a long period of time at considerable cost. Understandably the vendor regards this data as proprietary and seeks to control access by releasing only limited subsets specific to an application. In the early stages of a project, fluid properties and flow rates may not be well understood requiring repeated requests to the vendor for performance data which can be very time consuming. This reliance on vendor data that is not transparent does little to instil confidence in users who will often conduct costly independent trials to verify the suitability of the selected MPFM, or may revert to more conventional methods of measurement.

This paper presents an alternative analytical approach, developed for a heavy oil application in Alaska, providing an independent assessment of a Dual Gamma Venturi MPFM performance from the physical properties of the fluids and sensors. Phase and line density performance of the Dual Gamma phase detector sensor are examined with the phase calculations taking into account the phase densities, attenuation factors and detector count rates. Mass flow rate performance of the Venturi meter is examined for a high viscosity emulsion with Reynolds Number of less than 2,000 that requires a correction to the Venturi Coefficient of Discharge. Dual Gamma and Venturi performance are combined to find overall performance of the MPFM meter for comparison with the vendor data.

The "Analytical MPFM Performance" from the physical properties of the sensors and fluids goes hand-in-hand with the "Observational MPFM Performance" from comparative trials giving the user an immediate and independent verification of the MPFM performance. This speeds MPFM selection building confidence in the suitability of the MPFM and eliminating the need for costly and time consuming trials at calibration laboratories.

2 Introduction

A Fiscal measurement of heavy oil entering a common pipeline was required for allocation of exports to each pipeline entrant between the existing and new development. The economics of the development did not allow for processing the heavy oil to a suitable standard for measurement with a LACT unit. An alternative approach was required that

would be acceptable to the pipeline entrants, the Royalty Owners and regulatory authorities. As there was no field ownership overlap between the developments all parties will be fully exposed to the heavy oil measurement uncertainty however there is a fifteen to one difference in relative rates of production between the existing and new development reducing the existing producer's relative exposure proportionally. The heavy oil producer is subject to the full exposure arising from measurement which is offset against the much greater cost of processing to Custody Transfer standards.

Heavy oil with gravity of 19 to 21 ºAPI will be produced at up to 20,000 bpd from wells with ESP's (Electrical Submersible Pumps). With the expected water production the produced fluids will be a tight emulsion. The viscosity of the emulsion is dependant on water-cut and line temperature with a range of 50 to 10,000 cP with a temperature range of 60 to 120 ºF and WLR (Water Liquid Ratio) of 0 to 60 %v/v. Line pressure is 150 to 300 psig.

Figure 1 shows the configuration of the Heavy Oil Measurement comprising a slugcatcher to reduce emulsion slugging and to constrain gas in the liquid leg to a GVF (Gas Volume Fraction) of 0 to 60 %v/v for measurement with a Dual Gamma Venturi MPFM. Gas will be entrained in the emulsion, without slip between the phases, as a froth of small bubbles similar to bubbles in treacle and is not expected to form voids at lower GVF levels. This flow regime and the WLR and GVF range are well within the capabilities of the MPFM Dual Gamma phase detector. The Venturi flow element does pose some difficulties due to the high viscosity and therefore low Reynolds Number (Rn) in the laminar flow region that requires a correction to the venturi Coefficient of Discharge (Cd) constant. A two-path ultrasonic meter in the gas leg measures the gas produced to account for gas and entrained liquids and is not part of the Fiscal measurement.

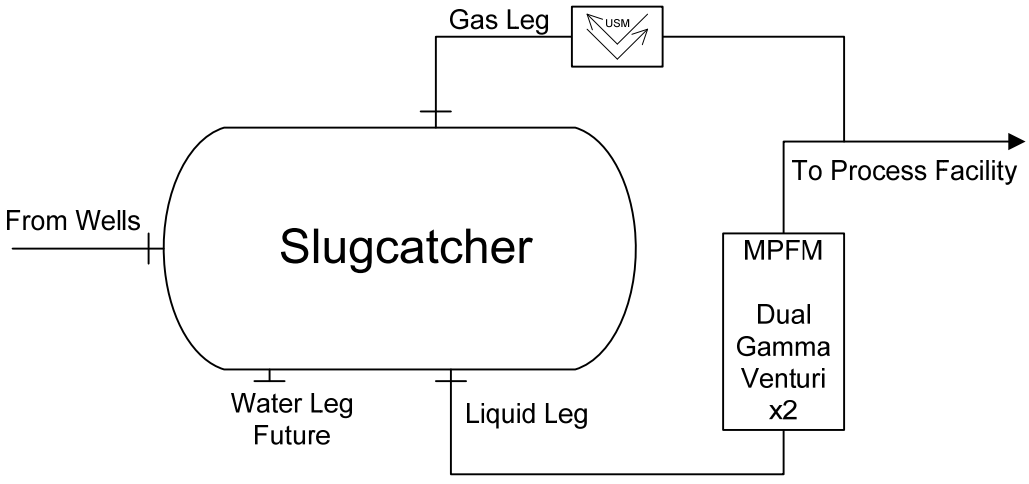

Figure 1 Heavy Oil Measurement

A model of the Dual Gamma Venturi MPFM phase detector and mass flow meter was developed to find the uncertainty and bias in the **oil standard volume Fiscal measurement**. The gas and produced water measurements in the Liquid Leg are not of interest for Fiscal measurement and are utilised as needed to implement the model.

The MPFM Model described in Section 3 includes a correction to the Venturi Cd constant for Rn based on published data, this being the main concern with the Heavy Oil measurement. The model is applied over the expected range of use to optimise the Venturi bore size selection for each of the two streams to minimise measurement uncertainty and cope with rapid changes in flow rate that arise due to slugging. This is achieved by switching the standby stream in or out of service as the flow rate changes to keep each MPFM within its optimum operating range, and maximise turndown.

The results for this application are discussed in Section 4, Conclusions including limitations of the current model and refinements to improve the model.

3 MPFM Model

The main components of the Dual Gamma Venturi MPFM shown in Figure 2 are:

1. Blind Tee — Mixer to improve the homogenous mixture of phases.
2. Venturi — Flow element with a calibrated bore and throat.
3. Temperature — Correction of oil volume to volume standard temperature.
4. Pressure — Correction of oil volume to volume at standard pressure.
5. Differential Pressure — Venturi ISO 5167 mass flow rate measurement.
6. Dual Gamma Detector — Measurement of WLR, GVF and mixture density.
7. Ambient Temperature — Dimensional correction.

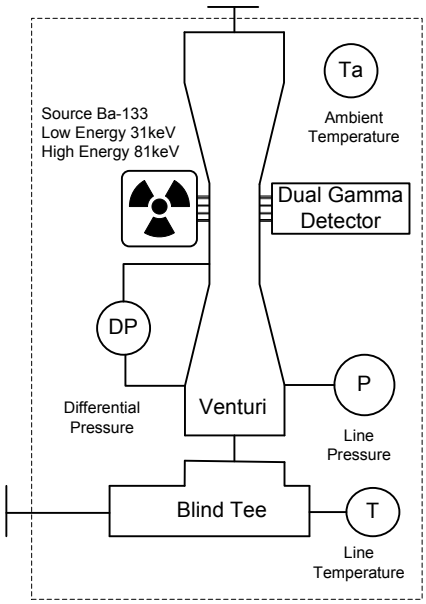

Figure 2 Dual Gamma Venturi MPFM

The MPFM model is constructed from a series of modules that calculate the measurement quantities, bias and uncertainty. Bias is found from duplicate calculations of the measurement quantities with the correct inputs and biased inputs respectively. Bias is found from the

difference between the results from the correct inputs and the biased inputs. By changing one input bias at a time the sensitivity of the measurement to each input can be found. Uncertainty is found with quadrature RSS (Root Sum Square) methods and MCS (Monte Carlo Simulation) methods in a hybrid RSS/MCS uncertainty model.

RSS is used for instrument measurements including line temperature, line pressure and venturi differential. RSS is also used to find the Venturi mass flow measurement using a modification to the orifice uncertainty method in ISO5167: 2003-2 [Ref. 5]. All other uncertainties are found by MCS including the API thermal and compressibility correction of oil volume from line to standard conditions and the AGA8 gas line density calculation, the Dual Gamma GVF, WLR and mixture density and the combination of all uncertainties. MCS takes account of all the dependencies and propagates uncertainty automatically eliminating the need to analyse the sensitivity of complex calculations. See "Uncertainty of Complex Systems by Monte Carlo Simulation" [Ref. 2] for explanation of MCS methods.

The MPFM modules are:

1.	Instrument Uncertainty	Differential Pressure, Static Pressure, and Temperature all by RSS.
2.	Line Conditions	Oil API thermal (Chpt. 11.1) and compressibility (Chpt. 11.2.1) correction for actual and standard density, Gas AGA8 actual density, Produced Water actual density from salinity all by MCS.
3.	Dual Gamma Phase	Uncertainty of GVF, WLR and Mixture Density from Oil, Gas and Produced Water actual density and mass attenuation with Low Energy and High Energy EPR (Empty Pipe Reference) count and Measurement count uncertainty all by MCS
4.	Venturi	Mass Flow calculation uncertainty from Mixture Density and Oil Standard Volume with a combination of RSS and MCS methods.
5.	Cd Correction	Reynolds Number found in the Venturi Module is used to find Cd from a correction curve for use in venturi mass flow calculation.
6.	Phase Envelope	Shows meter operating area and the mass attenuation factors limits.

The uncertainty and bias results are presented as three dimensional surfaces covering the GVF are WLR operating range in X-axis and Y-axis with the parameter of interest shown in the Z-axis. Figure 3 shows the Crude Oil Standard Volume Uncertainty surface for the conditions listed in Table 1. This includes the emulsion viscosity which increases with increasing water cut. The results at the four corners of the surface are summarised with other

results at the bottom of Table 1 which also shows bias due to oil and water input density bias discussed in the following sections.

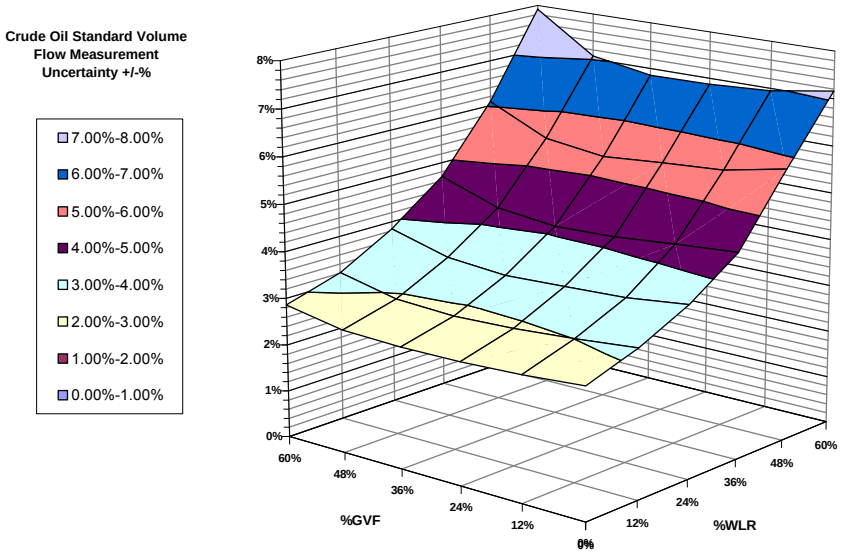

Figure 3 Crude Oil Standard Volume Uncertainty

Case	1			
Description	**Units**	**Measurement**	**Uncertainty**	**Bias**
Meter	Type	52mm		
Gamma Count Sample Rate	Seconds	40		
Liquid Line Flow Rate	bpd	20,000		
Gas Standard Density	SG	0.68	0.0023 lb/cf	0 lb/cf
Oil Standard Density	API°	20.6	0.58 lb/cf	1.87 lb/cf
Water Standard Density	lb/cf	64.30	0.32 lb/cf	1.87 lb/cf
Temperature	°F	78	0.45	
Pressure	psig	250.00	0.76	
Emulsion Viscosity	**%WLR**	**cP**		
	0%	121.00		
	12%	198.00		
	24%	361.00		
	36%	698.00		
	48%	1,806.00		
	60%	3,299.00		

Results	Units	GVF=0%, WLR = 0%	GVF=60%, WLR=0%	GVF=0%, WLR=60%	GVF=60%, WLR=60%
Oil Standard Volume Observed	stbpd	20,011	20,022	8,032	7,918
Oil Standard Volume Uncertainty	%	2.7%	2.8%	7.1%	7.6%
Oil Standard Volume Bias	%	-0.1%	-0.1%	-0.4%	-0.4%
GVF Observed	%GVF	-3.3%	58.7%	-3.1%	58.8%
GVF Uncertainty	%GVF	0.6%	0.5%	0.7%	0.5%
GVF Bias	%GVF	3.3%	1.3%	3.1%	1.2%
WLR Observed	%WLR	0.0%	0.0%	59.9%	59.9%
WLR Uncertianty	%WLR	1.0%	2.0%	1.5%	2.7%
WLR Bias	%WLR	0.0%	0.0%	0.1%	0.1%
Mixture Density Observed	kg/m^3	953.52	390.40	1,015.81	415.30
Mixture Density Uncertainty	%	1.1%	1.4%	0.9%	1.2%
Mixture Density Bias	%	-3.1%	-3.1%	-2.9%	-2.9%
Mixture Mass Flow Observed	kg/s	34.19	35.02	36.49	37.32
DP Observed	mbar	1515	3690	3108	5356
Viscosity Observed	cSt	131	53	3346	1339
Reynolds Number Observed		3459	21374	135	846
Discharge Coefficient Observed		0.932	0.955	0.672	0.819
Discharge Coefficient Uncertainty	%	2.164%	1.242%	5.960%	3.367%

Table 1 Crude Oil Standard Volume Conditions and Results with Bias

3.1 Dual Gamma GVF, WLR and Mixture Density

The proportions of oil, gas and water are found with a Dual Gamma detector which measures the attenuation of gamma counts from a Barium source at a Low Energy (31keV) and a High Energy (81keV) relative to an EPR (Empty Pipe Reference) count rate. The attenuation of the low energy source is predominantly dependant on the proportions of oil and water and the high energy source is predominately dependant on the proportion of liquid to gas although both count rates are affected to some degree by all phases.

The Phase Envelope in Figure 4 show linear mass attenuation for the full range of GVF from 0 to 100% and WLR from 0 to 100% in the outer triangle and the Heavy Oil MPFM range in the inner red triangle. The blue triangle illustrates the affect of undetected density bias discussed elsewhere. The corners of the triangle give the linear mass attenuation level single phase oil, gas and water.

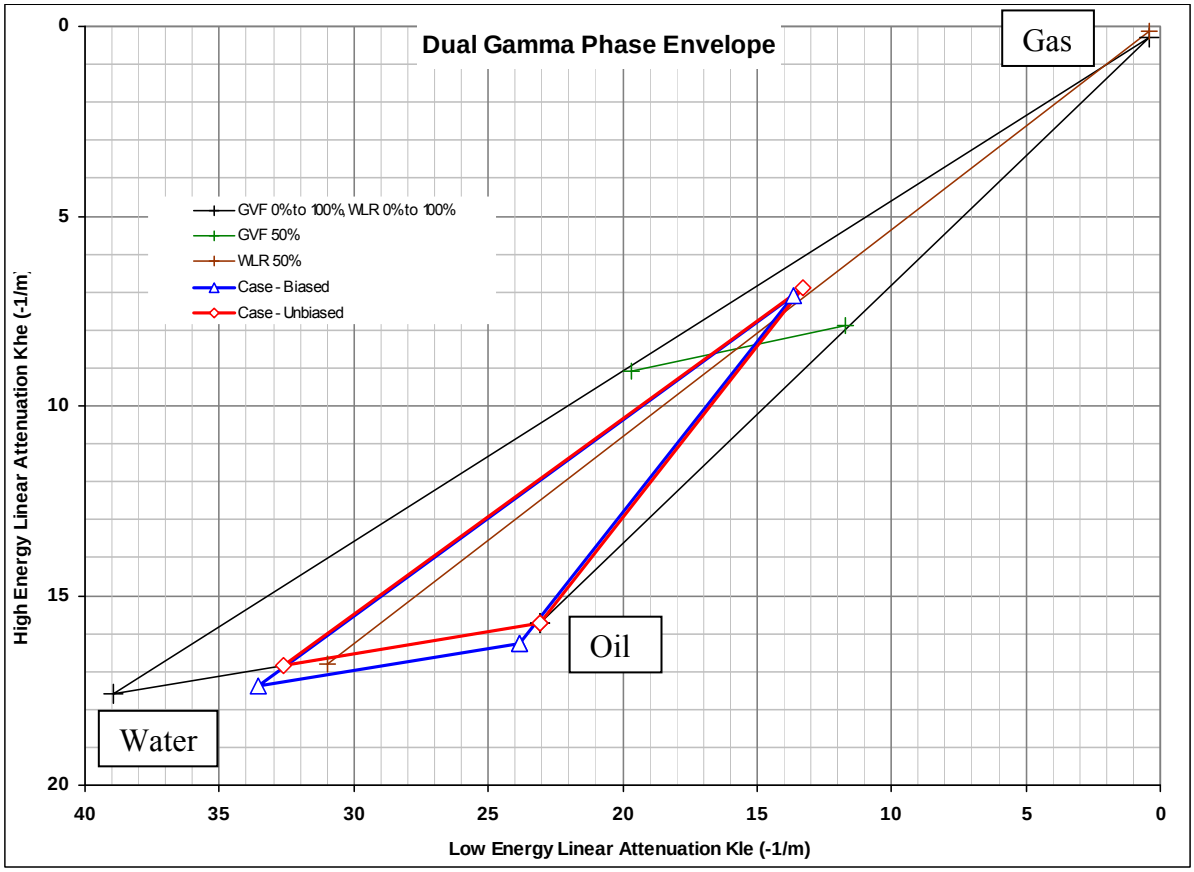

Figure 4 Phase Envelope

The attenuation can be found by calibration on actual fluid in single phase at each corner of the triangle or from the NIST X-Ray mass attenuation tables [Ref. 3] for the fluid composition.

The attenuation of gamma rays is dependant on the density of the mass attenuation coefficient of the penetrated material with the physical relationship:

$$N = N_o \cdot e^{-x\rho\mu}$$

where:

N	gamma detector count of the penetrated material
N_E	"empty pipe" gamma detector count
$x \cdot m$	gamma path length in metres
$\rho \cdot \frac{kg}{m^3}$	density of penetrated material in klogram per cubic metre
$\mu \cdot \frac{m^2}{kg}$	mass attenuation coefficient of penetrated material square meters per kilogram

Where the material is a mixture with oil, water and gas phases the equation is expressed as:

$$N = N_E \cdot e^{-x\left(\mu_o \cdot \rho_o \cdot \alpha_o + \mu_g \cdot \rho_g \cdot \alpha_g + \mu_w \cdot \rho_w \cdot \alpha_w\right)}$$

where:

α_{phase}	the fraction of oil, gas and water
$o \quad g \quad w$	subscripts identifying the oil, gas and water phases

The sum of the phase fractions is unity:

$$\alpha_o + \alpha_w + \alpha_g = 1$$

The detector has a low energy and high energy detection level which is expressed as:

$$N_{le} = N_{le0} \cdot e^{-x \cdot \left(\mu_{leo} \cdot \rho_o \cdot \alpha_o + \mu_{lew} \cdot \rho_w \cdot \alpha_w + \mu_{leg} \cdot \rho_g \cdot \alpha_g\right)} \quad \text{Low energy}$$

$$N_{he} = N_{he0} \cdot e^{-x \cdot \left(\mu_{heo} \cdot \rho_o \cdot \alpha_o + \mu_{hew} \cdot \rho_w \cdot \alpha_w + \mu_{heg} \cdot \rho_g \cdot \alpha_g\right)} \quad \text{High energy}$$

The equations can be represented in terms of linear attenuation constants for each energy:

$$K_{le} = \frac{\ln\left(\frac{N_{le}}{N_{le0}}\right)}{-x} = \mu_{leo}\cdot\rho_o\cdot\alpha_o + \mu_{lew}\cdot\rho_w\cdot\alpha_w + \mu_{leg}\cdot\rho_g\cdot\alpha_g$$

$$K_{he} = \frac{\ln\left(\frac{N_{he}}{N_{he0}}\right)}{-x} = \mu_{heo}\cdot\rho_o\cdot\alpha_o + \mu_{hew}\cdot\rho_w\cdot\alpha_w + \mu_{heg}\cdot\rho_g\cdot\alpha_g$$

The Dual Gamma Constant and Uncertainty Input in Table 2 lists all the inputs required to calculate Low Energy and High Energy counts over the required GVF and WLR range for input to the phase uncertainty module using the equations detailed above.

Dual Energy Gamma Densitometer – MCS Uncertainty					
Constants and Uncertainties					
Mixture	**Name**	**Units**	**Minimum**	**Maximum**	
Gas Volume Fraction	GVF	%gas/mix	0.0%	60.0%	
Water Liquid Ratio	WLR	%wtr/liq	0.0%	60.0%	
Density	**Name**	**Units**	**Value**	**Uncertainty**	**Bias**
Gas density	Rhog	kg/m^3	14.98	4.41%	0.00
Oil density	Rhoo	kg/m^3	923.7	1.00%	30.00
Water density	Rhow	kg/m^3	1027.3	1.00%	30.00
Gamma Detector	**Name**	**Units**	**Value**	**Uncertainty**	**Bias**
Path length	x	m	0.052	0.010%	0.00000
Low Energy	**Name**	**Units**	**Value**	**Uncertainty**	**Bias**
EPR Count Rate	Nle0	Hz	24,109.7	1.46	0.00
EPR Ave. Period	tle0	Sec	43,200		
EPR Samples	Sle0		1		
Measurement Count	mtle	Hz			0.00
Measured Ave. Period	tle	Sec	40		
Measured Samples	Sle		1		
Gas attenuation	Muleg	m^2/kg	0.025830400	0.50%	0.0000000
Oil attenuation	Muleo	m^2/kg	0.024967800	0.50%	0.0000000
Water attenuation	Mulew	m^2/kg	0.037914000	0.50%	0.0000000
High Energy	**Name**	**Units**	**Value**	**Uncertainty**	**Bias**
EPR Count Rate	Nhe0	Hz	12,541.4	1.06	0.00
EPR Ave. Period	the0	Sec	43,200		
EPR Samples	She0		1		
Measurement Count	mthe	Hz			0.00
Measured Ave. Period	the	Sec	40		
Measured Samples	Sle		1		
Gas attenuation	Muheg	m^2/kg	0.018003700	0.50%	0.0000000
Oil attenuation	Muheo	m^2/kg	0.017045900	0.50%	0.0000000
Water attenuation	Muhew	m^2/kg	0.017131700	0.50%	0.0000000

Table 2 Dual Gamma Constant and Uncertainty Input

The table includes the inputs for bias to enable investigation bias in the results arising from bias in the inputs. In the example the oil and water densities both have a +30kg/m3 bias. The effect of this can be seen in the Phase Envelope in Figure 4 which shows the linear attenuation bias in blue causing the small bias in Table 1, Crude Oil Standard Volume Conditions and Results with Bias illustrates relatively low sensitivity to large oil and water density biases. Other work has shown that oil density bias due to a change in the hydrocarbon composition has little effect on the oil mass attenuation factor. Small changes in the produced water density due to changes in salinity have a corresponding bias in the mass attenuation factor increasing the overall the WLR bias and dependant calculations.

Table 2 also shows the EPR and Measurement count rates including sampling intervals. The EPR is sampled for 12 hours to minimise the reference count uncertainty which is found from the square root of the number of counts divided by the count period in seconds to find the uncertainty in counts per second. It is also essential that the MPFM conditions are kept constant for this period of time. The Measurement count uncertainty is found in the same way however the count averaging period of forty seconds is chosen so the uncertainty is greater.

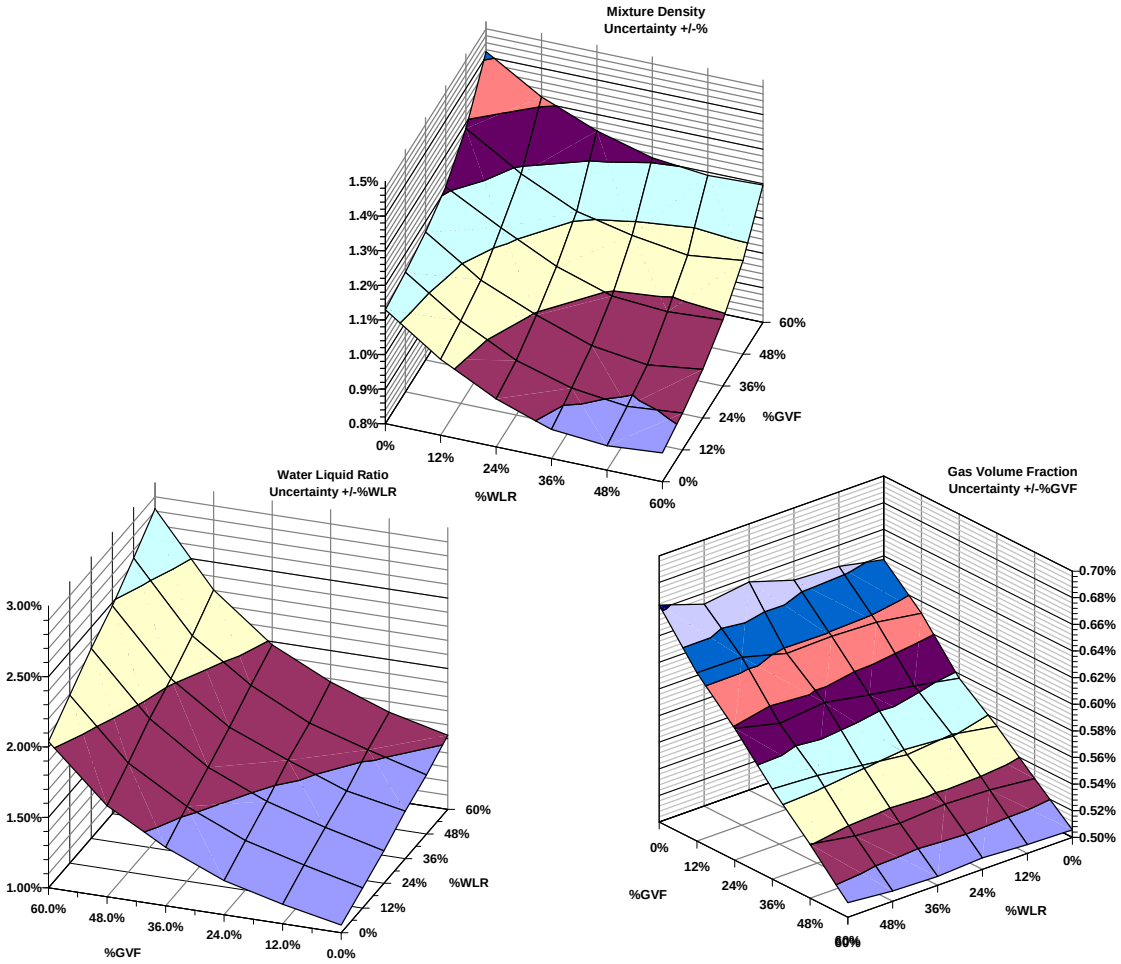

Figure 5 Dual Gamma WLR, GVF and Mixture density Uncertainty

Using the input data the uncertainty is calculated by MCS to find the Dual Gamma WLR, GVF and Mixture density Uncertainty surfaces shown in Figure 5 on the next page.

Oil, produced water and gas densities are calculated in the Line Condition module for use in the Dual Gamma module and Venturi module. Oil density is corrected to standard conditions using the API thermal and compressibility methods. Water density is calculated from the salt content and the gas densities are calculated from a gas composition using AGA8. Uncertainty is found with MCS for all densities. Pressure and temperature measurement uncertainties found by RSS are taken from the Instrument module. Table 3 shows the inputs, densities and uncertainty results for the Line Conditions module.

Fluid	Quantity	Name	Unit	Value	Uncertainty	
Conditions	Temperature	Tmix	°F	78.0		
			°C	25.56	0.45	
	Pressure	Pmix	psig	250.00		
			barg	17.042	0.76	
Oil	Gravity	APIoil	°API	20.6		
	Standard Density	ρsoil	kg/m^3	929.39		
	Vapour Pressure	Pvap	psig	10.00		
			barg	0.68		
	Thermal Correction	Ctloil	factor	0.992877		
	Pressure correction	Cploil	factor	1.001022		
	volume correct.	VCFoil	factor	0.993891		
	actual density	ρaoil	kg/m^3	923.71		
	standard volume correction factor			0.993891	0.10%	0.99399971
Water	standard density	ρswtr	kg/m^3	1,030.030		
	salinity		kg/kg	0.0429196		
	actual density	ρawtr	kg/m^3	1,027.319		
	standard volume correction factor			0.997368	0.10%	0.997866191
Gas	standard density	ρsgas	kg/m^3	0.83107		
	actual density	ρagas	kg/m^3	14.985		
	dyn. viscosity	μgas	cP @60°F	0.015		
	kin. viscosity	νgas	cSt	1.00102		
AGA8 Gas Density						
Line Conditions	**Measurement**	**Uncertainty**				**Trial Values**
Temperature deg C	25.56	0.450				25.43
Pressure bara	18.05	0.755				18.40
Gas Composition	**Compostion mol%**	**Normalised mol%**	**Component Uncertainty %**	**Uncertainty mol%**	**Trials**	**Normalised Trials**
Nitrogen mol%	0.720	0.720	1.00%	0.0072	0.7185	0.7174
Carbon Dioxide mol%	1.360	1.360	1.00%	0.0136	1.3676	1.3655
Methane mol%	85.330	85.330	2.00%	1.7066	85.4663	85.3403
Ethane mol%	6.150	6.150	1.00%	0.0615	6.1468	6.1377
Propane mol%	3.810	3.810	1.00%	0.0381	3.8206	3.8150
n-Butane mol%	2.020	2.020	1.00%	0.0202	2.0175	2.0145
i-Butane mol%	0.000	0.000	1.00%	0.0000	0.0000	0.0000
n-Pentane mol%	0.580	0.580	1.00%	0.0058	0.5807	0.5799
i-Pentane mol%	0.000	0.000	1.00%	0.0000	0.0000	0.0000
n-Hexane mol%	0.030	0.030	1.00%	0.0003	0.0297	0.0297
n-Heptane mol%	0.000	0.000	1.00%	0.0000	0.0000	0.0000
n-Octane mol%	0.000	0.000	0.00%	0.0000	0.0000	0.0000
n-Nonane mol%	0.000	0.000	0.00%	0.0000	0.0000	0.0000
n-Decane mol%	0.000	0.000	0.00%	0.0000	0.0000	0.0000
Total mol%	100.000	100.00			100.15	100.00
Normalised	**True Result**	**Method Uncertainty**	**MCS Mean**	**MCS Uncertainty**	**Trials with Method**	**Trials**
Line Density Kg/m3 (AGA8)	14.98	0.10%	14.98	4.41%	15.29	15.29
Standard Density Kg/m3 (AGA8)	0.8311	0.10%	0.83	0.34%	0.8310	0.8310
Line/Standard	18.03		18.02	4.40%	18.40	18.40

Table 3 Line Conditions Density Uncertainty

3.2 Venturi Mass Flow Rate

3.2.1 Venturi Method

The Venturi mass flow rate is calculated in accordance with ISO5167-4 [Ref. 6] and the uncertainty is calculated using a modified orifice uncertainty in ISO5167-2 [Ref. 5] which takes into account uncertainty in Cd, expansion factor, bore diameter, throat diameter, differential pressure uncertainty and the mixture density uncertainty from the Dual Gamma phase detector. In the model the mass flow rate is known enabling the calculation of the differential pressure for each GVF and WLR point with an inverse venturi calculation.

The model flow rates are for a constant Liquid Standard Volume which in this example is 20,000 stbpd therefore the line volume flow rates will vary with GVF and WLR with higher fluid velocity at high GVF resulting in high differential pressure with a 4:1 over the GVF, WLR range.

3.2.2 Cd (Coefficient of Discharge) Correction

Cd is dependant on Rn (Reynolds Number) which is found from the Velocity and the Kinematic Viscosity of the fluid and the bore diameter of the meter. Viscosity is dependant on the WLR of the emulsion. The viscosity may also be dependant on the GVF and has been combined in proportion to the GVF to find the viscosity of the mixture. Figure 6 shows the wide variation in viscosity over the operating range of the meter from 53cSt at WLR=0%, GVF=60% to 3,346 at WLR=60% and GVF=0%.

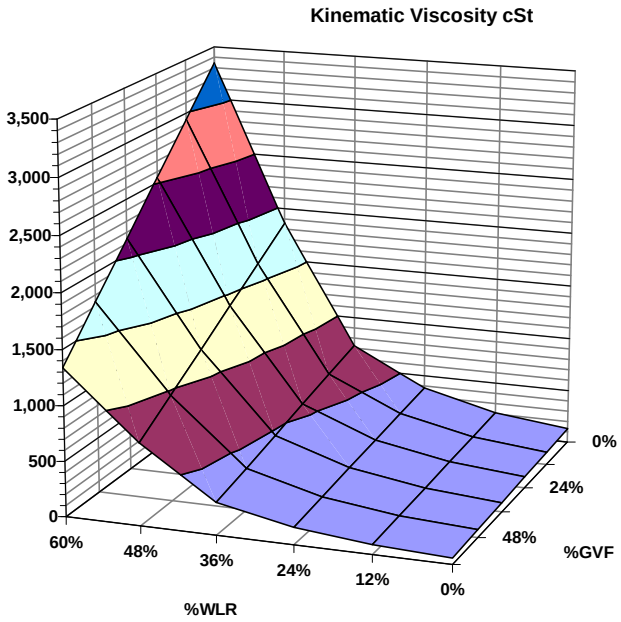

Figure 6 Viscosity Variation

The viscosity variation results in Reynolds Number range 135 to 21,374 in Figure 7.

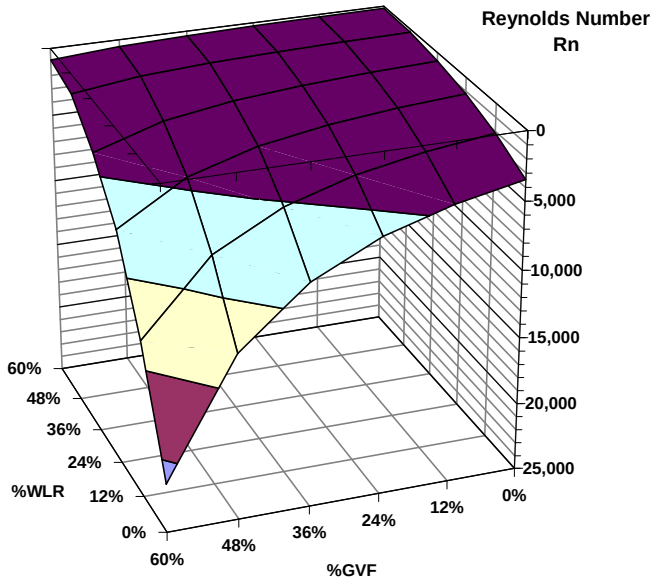

Figure 7 Rn Variation

At Rn below 10,000 the fluid is in transition from turbulent flow with a repeatable Cd= 0.95 to laminar flow with Rn progressively falling to 0.6 shown in Figure 8 below.

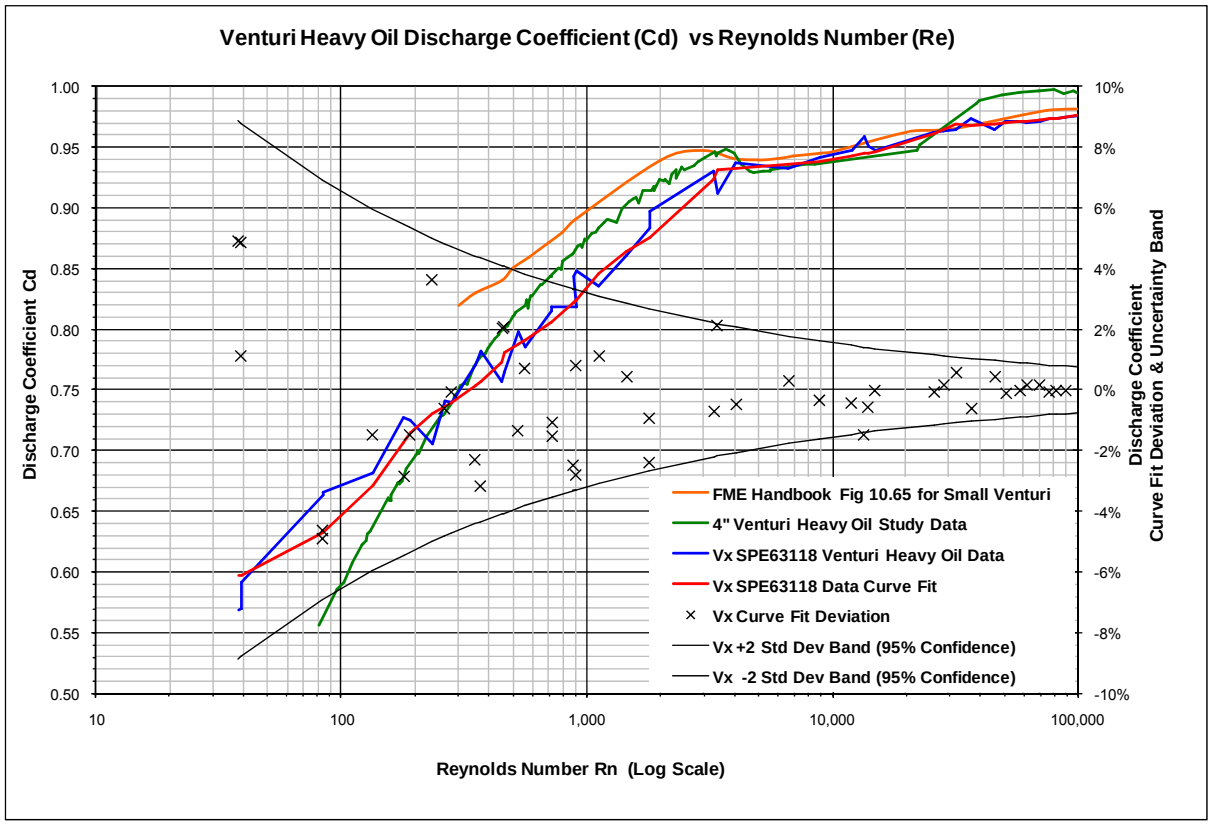

Figure 8 Change in Discharge Coefficient (Cd) with Reynolds Number (Rn)

Coefficient of Discharge (Cd) used in the Venturi equation is found from a Rn vs. Cd look-up table which is plotted as the red trace in Figure 8. This is a curve-fit of the data from the Heavy Oil MPFM paper SPE63118 [Ref.1] shown in the blue trace. This curve compares well with 4" Venturi Heavy Oil SWRI study data [Ref. 11] shown in the green trace and the orange trace from Figure 10.65 of the Flow Measurement Engineering Handbook [Ref. 10].

Data points "x" in Figure 8 are the deviation between the original SPE63118 data and the corresponding curve-fit point. The "trumpet" curve in Figure 8 is found from twice the standard deviation (95% confidence interval) of the "x" data points which represents uncertainty of the curve-fit. The uncertainty of Cd was taken from the curve-fit variability for the SPE63118 Heavy Oil data which did not have a stated uncertainty. The uncertainty is of a similar order to the FME data of ±2%OMV where the traces overlap. This increases to ±8%OMV at the lowest Rn. The Coefficient of Discharge (Cd) and Uncertainty (UCd) surfaces are shown in Figure 9 for the WLR and GVF in earlier examples.

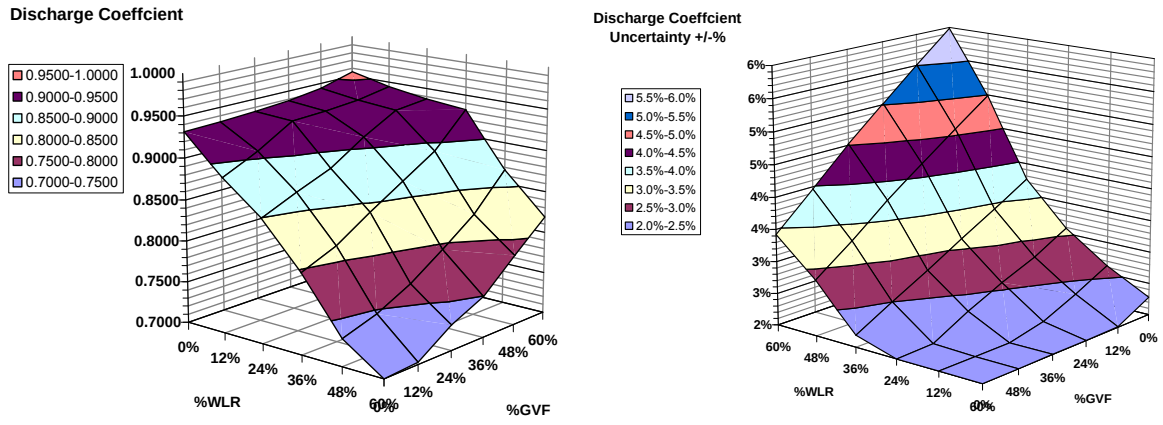

Figure 9 Coefficient of Discharge (Cd) and Uncertainty (UCd)

3.3 Combined Standard Volume

The Dual Gamma GVF, WLR, mixture density and Venturi mass flow rates are combined to calculate the Oil Standard Volume and Uncertainty as follows:

1. Mixture volume mixture mass flow divided by mixture density

   $Qv_{mix} = Qm_{mix} / \rho_{mix}$

2. Oil line volume is found from GVF and WLR

   $Qv_{oil} = Qv_{mix} \times GVF \times (1\text{-}WLR)$

3. Oil standard volume found from the API thermal and compressibility corrections

   $Qstdvol_{oil} = Qv_{oil} \times Ctl_{oil} \times Cpl_{oil}$

The uncertainty is found by propagating the uncertainty for each measurement through these calculations using MCS (Monte Carlo Simulation).

The Propagation of Uncertainties are summarised in Figure 10 below showing that high viscosity is the dominant influence on uncertainty with Heavy Oil due to low Reynolds Number and so Coefficient of Discharge.

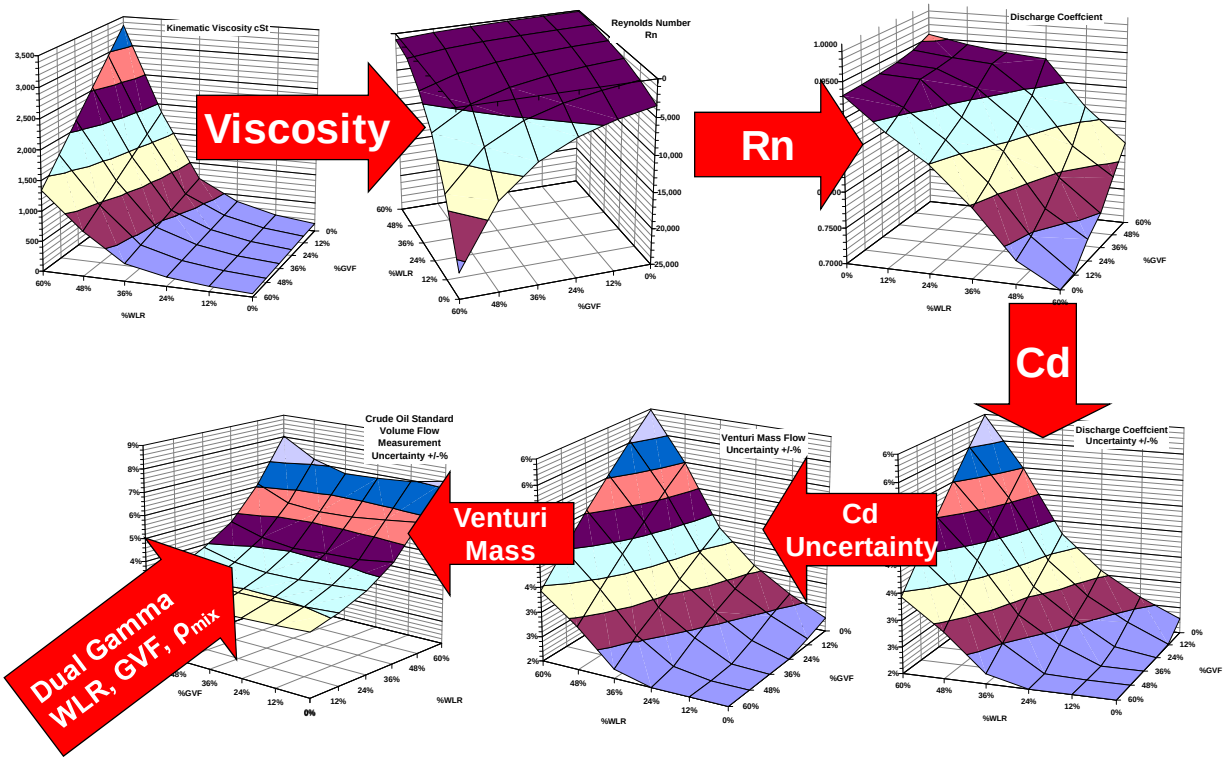

Figure 10 Propagation of Uncertainties

4 Conclusions

The Crude Oil Standard Volume Uncertainty for the base case in Figure 3 of ±3%OMV was within ±0.5%OMV of the vendor's uncertainty over the full GVF range from 0 to 60% for WLR from 0 to 12%. For WLR's above 12% the influence of the increase in the increasing viscosity of the emulsion with WLR and its influence on Reynolds Number and Coefficient Discharge do not appear to have been taken into account and the results diverged with a maximum difference of ±5%OMV at a WLR of 60%. Other documentation from the vendor and the SPE63118 paper [Ref. 1] has taken the increase in the oil measurement uncertainty due to viscosity into account and is of the order of ±5%OMV at a WLR of 60% whereas the model showed an uncertainty of ±8%OMV.

The model proved to be valuable in understanding bias due to produced water salinity variation which affects the density and mass attenuation factor additively whereas variation in oil composition impacts the oil density but has a negligible impact on the mass attenuation

factor so a relatively large oil density bias can be tolerated which has implication for sampling and analysis of oil and produced water.

The primary advantage of a model was the ability to evaluate the feasibility of various measurement options at each stage of production throughout the field life and when production conditions change. This enabled the selection of meter size, DP span and the number of meters for forecast production rates to be examined to find the optimum configuration.

The mass attenuation factors for oil, produced water and gas for this project were calculated in a separate mass attenuation model based on composition using NIST data [Ref. 3]. This was a great advantage for this project as the fluid properties were known from reservoir samples but samples were not available to measure the mass attenuation. The model could be improved incorporating the mass attenuation into the MPFM model to automate the mass attenuation calculation.

Whilst trials at a calibration facility do provide valuable information the production conditions can not be duplicated and the trials will only provide a rough indication of the meter performance. This also applies to observational data which is dependant on how well the observational data is matched to forecast and actual production conditions. A physical model also has limitations being dependant on knowledge of the production conditions and fluid properties which may be limited at the early stages of a project. As a project progresses knowledge of these conditions is gained and the model can be refined to provide an improved uncertainty prediction which can be used throughout the field life.

5 References

1. Atkinson, D. I., et al., "Qualification of a Nonintrusive Multiphase Flow meter in Viscous Flow", SPE63118, 200 SPE Annual Technical Conference and Exhibition, Dallas, TX, October 1-4, 2000.
2. Basil, M., Jamieson, A. W., "Uncertainty of Complex Systems by Monte Carlo Simulation", 16th North Sea Flow Measurement Workshop, Gleneagles, 26th to 29th October 1998.
3. Hubbell, J. H., Seltzer, S. M., Tables of X-Ray Mass Attenuation Coefficients and Mass Energy-Absorption Coefficients, National Institute of Standards and Technology, April 1996.
4. ISO 5167-1: 2003(E), Measurement of fluid flow by means of pressure differential devices inserted in circular cross-section conduits running full -Part 1: General principles and requirements
5. ISO 5167-2: 2003(E), Measurement of fluid flow by means of pressure differential devices inserted in circular cross-section conduits running full -Part 2: Orifice plates
6. ISO 5167-4: 2003(E), Measurement of fluid flow by means of pressure differential devices inserted in circular cross-section conduits running full -Part 4: Venturi tubes

7. ISO 5168: 2005(E),, Measurement of fluid flow – Procedures for the evaluation of uncertainties
8. ISO/IEC Guide 98: 1995, 2nd Edition; Guide to the expression of uncertainty in measurement (GUM).
9. ISO/IEC NP Guide 98: 1995/DSuppl 1.2, Propagation of distributions using a Monte Carlo method.
10. Miller, R. W., Flow Measurement Engineering Handbook, McGraw-Hill, New York, 1996, 3rd Edition: Page 10.63, Figure 16.5 Discharge coefficient for venturi.
11. Stobie, G. S., et al., "Erosion in a Venturi Meter with Laminar and Turbulent Flow and Low Reynolds Number Discharge Coefficient Measurement", 25th International North Sea Flow Measurement Workshop, October 16-19, 2007 Oslo, Norway.

6 Acknowledgement

Dr Andrew Hall's assistance with mass attenuation calculations was greatly appreciated.